J. Biomater. Sci. Polymer Edn, Vol. 18, No. 12, pp. 1575–1589 (2007)

Also available online - www.brill.nl/jbs

Investigation on the properties of methoxy poly(ethylene glycol)/chitosan graft co-polymers

LIANDONG DENG, HAIYING QI, CHUNMEI YAO, MENGHUANG FENG and ANJIE DONG *

Department of Polymer Science and Technology, School of Chemical Engineering and Technology, Tianjin University, Tianjin, 300072, China

Received 22 November 2006; accepted 30 April 2007

Abstract—Methoxy poly(ethylene glycol)/chitosan graft co-polymers (CS-g-mPEGs) with different degrees of substitution were synthesized by reductive *N*-alkylation of chitosan with poly(ethylene glycol) aldehyde. The crystalline and thermal properties of CS-g-mPEGs were characterized by wide-angle X-ray diffraction (XRD), differential scanning calorimetry (DSC) and thermogravimetry (TG). The results indicate that CS-g-mPEG solids represent microphase separation morphology with mPEG crystal and CS domains coexistence and the introduction of PEG on CS improves the thermal decomposition. The hydrodynamic behavior of CS-g-mPEGs in aqueous solution and the influence of NaCl were investigated. The results indicate that the hydrodynamic behavior of CS-g-mPEGs in aqueous solution is significantly affected by the degree of substitution and the concentration of NaCl, which are quite different from that of CS. The results of this paper also certify that CS-g-mPEGs keep the property of complexation with a counter-ion, such as tripolyphosphate, to form nanoparticles through the electrostatic interaction.

Key words: Chitosan; methoxy poly(ethylene glycol); graft co-polymers; nanoparticles; hydrodynamic behavior.

INTRODUCTION

Chitosan, a non-toxic, biocompatibility and biodegradable polysaccharide and cationic polyelectrolyte, derived from chitin, a naturally abundant material found in the shells of crustaceans, has shown some favorable biological activities, such as immunological, anti-bacterial and wound healing activity. Chitosan has many biomedical applications [1–4], especially as the biomaterial for the delivery and control release of gene, vaccines and proteins [5, 6]. However, the poor solubility

*To whom correspondence should be addressed. Tel.: (86-22) 2789-0706; Fax: (86-22) 2789-0710; e-mail: ajdong@tju.edu.cn

of chitosan in water and organic solvents limits its effective application. Various chitosan derivatives have been prepared by chemical modification to overcome this disadvantage and generate new biofunctional materials [7, 8], among which chemical modification of chitosan with poly(ethylene glycol) (PEG) is considered to be a convenient way to improve the biocompatibility and water solubility of chitosan [9–14]. PEG has been widely used in modification of biomaterials because of its outstanding physico-chemical and biological properties, including flexible, hydrophilicity, lack of toxicity, ease of chemical modification, absence of antigenicity and immunogenicity, biocompatibility and steric repulsion.

To date, several kinds of CS-g-PEG productions have been synthesized through different chemical modification ways by using PEG and PEG derivatives [14–22], such as PEG-ester [14], PEG-sulfonate [15], PEG-acid [16], PEG-aldehyde [17], PEG-acrylate [18] and PEG-iodide [19]. Various reports have been published related to the water solubility and bioactivity of CS-g-PEGs and the results show that conjugation of PEG to chitosan not only can enhance water solubility and biocompatibility of chitosan, but also favorably provide further biological functionality to improve the bioavailability of drug *in vivo* [15, 18, 23–30]. The unmodified glucosamine units of CS-g-PEGs still keep their intrinsic properties as found in native chitosan, such as aggregation by strong inter- or intra-molecular hydrogen bonds, interaction with other glucosamine units and complexation by electrostatic interaction with negative charged compounds, which afford CS-g-PEGs potential application in drug delivery. Nanoparticles of chitosan with sodium tripolyphosphate ionic gel have been used as drug-delivery carriers [31–35]. Chitosan complexes with proteins and genes are also thought as suitable carriers for biomolecules [36–41]. The influences of molecular weight, deacetylation degree, concentration of chitosan and PEG introduction on the drug-delivery properties have been studied [34]. The formation of chitosan–DNA complex nanoparticles and the effect of PEGylation have also been investigated [37, 38]. It has been found that PEG conjugation can improve the physical–chemical stability and storage stability of chitosan–DNA complex nanoparticles, and more importantly the PEGylation can decrease the toxicity of chitosan nanoparticles, but does not affect the transfection potency, DNA conformation and chitosan's DNA binding ability. Ouchi *et al.* investigated the aggregation phenomena of PEG-grafted chitosan in aqueous solution through light scattering measurements [17]. CS-g-PEGs can spontaneously form nanometer-sized aggregates by strong intermolecular hydrogen bonds between the chitosan moiety in water and the compact aggregates are formed by CS-g-PEGs with higher content of PEG. The CS-g-PEG aggregates can take up a small hydrophobic molecule such as N-phenyl-1-naphthylamine (PNA) and release PNA by changing the pH to an acidic condition. The hydrodynamic properties of CS-g-PEGs will affect the aggregation behavior of CS-g-PEGs with oppositely charged molecules, but there are only few reports on the properties of CS-g-PEG aqueous solution, except for the water solubility [21–23]. In this paper, the hydrodynamic properties and aggrega-

tion behavior of CS-g-PEGs in aqueous solution were studied by combination of crystalline and thermal properties characterization.

MATERIALS AND METHODS

Materials

Chitosan (CS) with a deacetylation degree of 92.5 mol% sugar/unit and a number-average molecular mass of 56 kDa was obtained from Yuhuan Ocean Biochemical (Zhejiang, China). Methoxy poly(ethylene glycol) (mPEG, 2 kDa) was purchased from Aldrich (St. Louis, MO, USA). Other reagents were all analytical grade and used without further purification.

Preparation of mPEG-aldehyde

mPEG-aldehyde (mPEG-CHO) was prepared by the oxidation of mPEG with anhydrous dimethylsulfoxide/acetic anhydride [23, 24]. Acetic anhydride (10.2 ml) was added to mPEG (20 g) in 60 ml anhydrous dimethylsulfoxide containing 4 ml chloroform under a N_2 atmosphere and the mixture was stirred for 9 h at 20°C. The reaction mixture was then poured into 400 ml anhydrous diethyl ether. The precipitate was filtered with a paper filter (No. 2) and re-precipitated twice from chloroform solution with diethyl ether. The precipitate was dried under vacuum for 24 h. The degree of conversion (DC) from hydroxyl group to aldehyde group was estimated by the hydroxylamine method and the DC was 60%. The unreacted mPEG does not affect the synthesis and properties of CS-g-mPEG.

Preparation of CS-g-mPEGs

CS-g-mPEGs was prepared by the method of Bentley *et al.* [24]. Chitosan (0.25 g, 1.4 mmol monosaccharide residue containing 1.3 mmol amino group) was dissolved in a mixture of 2% acetic acid solution (10 ml) and methanol (5 ml). 3 ml mPEG-CHO aqueous solution (1.25 g, –CHO 0.375 mmol) was added to the above chitosan solution and stirred for 30 min at room temperature. Then the pH of the Chitosan/mPEG-CHO solution was adjusted to 6.5 with 1 mol/l NaOH solution and stirred for 60 min at room temperature. $NaCNBH_3$ ($NaCNBH_3$/CHO of mPEG $= 10:1$ mol/mol) was added to the reaction mixture and the solution was stirred for 24 h at room temperature. The reaction mixture was dialyzed with a dialysis membrane (12 kDa molecular mass cut-off) against water for 72 h and the unreacted mPEG was removed. The dialyzed solution was centrifuged by a centrifuger (LD5-2A, Beijing, China) at 5000 rpm for 15 min. The supernatant was frozen and lyophilized by a freeze dryer system (LGJ-10, Four-Ring Science Instrument Plant, Beijing, China) and then washed twice with 100 ml acetone. The unreacted mPEG was removed again by washing with acetone. After drying *in vacuo*, the obtained white powder was CS-g-mPEGs. The reaction conditions and

Table 1.
Preparation of CS-g-mPEG[a]

Run No	Molar ratio		CS-g-mPEG		
	–CHO of mPEG[b]/–NH_2 of chitosan	$NaCNBH_3$/–CHO of mPEG	Yield[c] (wt%)	DS[d] (%)	CS (wt%)
CS-g-mPEG1	0.05	10	21	6	57
CS-g-mPEG2	0.10	10	27	14	36
CS-g-mPEG3	0.15	10	38	18	30
CS-g-mPEG4	0.20	10	49	22	27

[a] Chitosan (5.6 kDa, degree of deacetylation 92.5%) was obtained from Yuhuan Ocean Biochemical. Reaction conditions: a mixture of 2% acetic acid and methanol was used as solvent, pH was 6.5, reaction temperature was room temperature and the reaction time was 24 h.

[b] The –CHO content is 60 mol% and –CHO is estimated by the hydroxylamine method.

[c] Yield is defined as the amount of recovered chitosan in mPEG-g-CS calculated by DS.

[d] DS means the degree of substitution of mPEG to monosaccharide residue of chitosan determined with a Carlo Erba 1106 element analyzer.

the degree of substitution (DS) of mPEG to monosaccharide residue of chitosan as measured using a Carlo Erba 1106 element analyzer are shown in Table 1.

Hydrodynamic studies

A series of CS-g-mPEG aqueous solutions with deionized H_2O (pH 6.0) or 2% acetic acid (pH 2.0) aqueous solution as the solvent was prepared. The reduced viscosities (η_{sp}/C) of CS-g-mPEGs in aqueous solutions were measured by an Ubbelohde viscometer at 30°C as shown in equation (1). The effects of the NaCl concentration (C_{NaCl}) on η_{sp}/C of CS-g-mPEGs in acetic acid solution were also investigated at a polymer concentration of 10 mg/ml.

$$\eta_{sp}/C = \left(\frac{t}{t_0} - 1\right)\Big/C, \tag{1}$$

where t_0 is the time that the solvent flows out of the Ubbelohde viscometer, t is the time that the polymer solution flows out of the Ubbelohde viscometer and C is the concentration of polymer solution.

Preparation of nanoparticles

The CS-g-mPEG nanoparticles (NPs) were prepared by ionic gelation using sodium tripolyphosphate as cross-linker. CS-g-mPEGs (20 mg) was dissolved in 2% acetic acid solution (2 ml) and this solution was dropped into the sodium tripolyphosphate solution under magnetic stirring at ambient temperature for 10 min. The mixture was dialyzed with a dialysis membrane (12 kDa molecular mass cut-off) against water for 48 h. The dialyzed solution was frozen and lyophilized to obtain the NPs powder. The freeze-dried powder could be dispersed in water.

Characterization

The compositions of CS-g-mPEGs were measured in D_2O solutions by proton nuclear magnetic resonance spectroscopy (^{1}H-NMR). The ^{1}H-NMR measurements were carried out on 500 MHz Varian Unity Plus INOVA 500 with tetramethylsilane (TMS) as the internal standard at 25°C.

DS of CS-g-mPEGs was measured by a Carlo Erba 1106 element analyzer and was calculated using equation (2).

$$\mathrm{DS} = \frac{\mathrm{C/N}}{77.42} \times 100\%, \tag{2}$$

where C and N is the content (wt%) of carbon and nitrogen element in CS-g-mPEGs, respectively, and 77.42 is the C/N value at DS of 100 mol%, at which all the amine groups in chitosan are substituted by mPEG.

Wide-angle X-ray diffraction (XRD) patterns were recorded with graphite-filtered Cu Kα radiation produced with a BDX3300 diffractometer (Beijing university instrument manufacture, China). All the samples were measured at a voltage of 20 kV, current of 20 mA, scan range of 3–45° and scan interval of 0.0334°.

Differential scanning calorimetry (DSC) measurements were carried out with Diamond DSC (Perkin Elmer, Norwalk, CT, USA). All the samples were approximately 5 mg. All the measurements were carried out at a heating (cooling) rate of 10°C/min from −50 to +200°C.

The thermal weight-loss analyses of chitosan and CS-g-mPEGs were carried out with a thermogravimetric apparatus (Perkin Elmer Pyris 6 TGA) at a heating rate of 10°C/min. All the samples were approximately 11 mg.

The size and distribution of the CS-g-mPEG NPs were determined using a BI-90Plus laser particle size analyzer (LPSA, Brookhaven Instruments, Brookhaven, CT, USA). For all cases, λ was 678 nm, the angle of measurement was 90° and the temperature was 25°C.

Zeta potential of CS-g-mPEGs in aqueous dispersions was determined using a BI-Zeta Plus zeta potential analyzer (Brookhaven Instruments).

The transmission electron microscopy (TEM) specimens for the CS-g-mPEG NPs dispersion were observed under a JEM-100CX II instrument. The samples were prepared by adding a drop of the CS-g-mPEG NPs dispersion on the Formvar-coated copper TEM grid, and then dyed with phosphatotungstic acid.

RESULTS

^{1}H-NMR analysis of CS-g-mPEGs

The structure of CS-g-mPEGs is shown in Scheme 1 and the peaks assigned to protons of the chitosan and mPEG units can be observed in Fig. 1. Compared to chitosan [42], the peaks corresponding to –$NHCH_2$ (Fig. 1, peak e) and CH_2O– (Fig. 1, peak d) appear at 2.6 and 3.70 ppm on the ^{1}H-NMR spectrum of CS-g-mPEGs. The

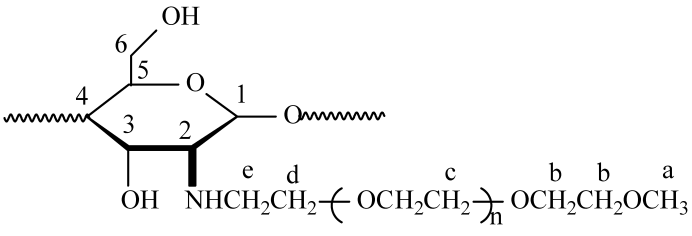

Scheme 1. Structure of CS-g-mPEGs.

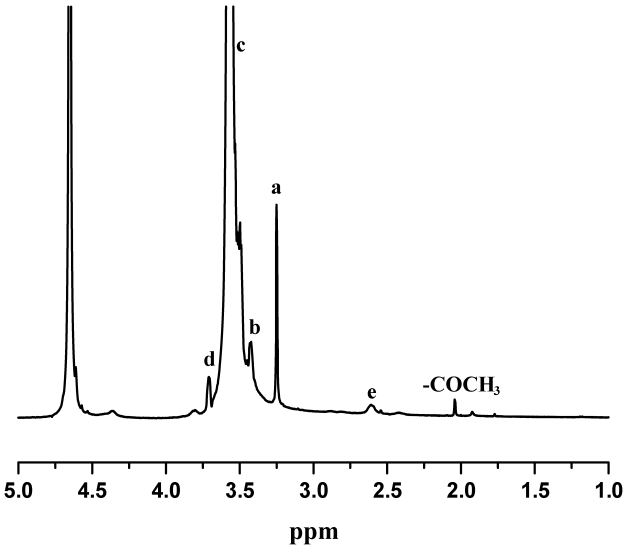

Figure 1. ^{1}H-NMR spectrum of CS-g-mPEG (DS = 20%). The ^{1}H-NMR measurements were carried out on a 500 MHz Varian Unity Plus INOVA 500 with tetramethylsilane (TMS) as the internal standard at 25°C.

sharp single signal at 3.25 ppm is assigned to $-OCH_3$ (Fig. 1, peak a) of mPEG units and the peak at 2.04 ppm assigned to $-COCH_3$ of the *N*-acetylglucosamine units. The peak of PEG methylene (3.57 ppm, H, Fig. 1, peak c) overlaps with those of H-3, 4, 5, 6 and 1 of the glucosamine units, so it cannot be distinguished. The peak of H-2 is too weak to appear. The results show that the structure of the graft co-polymer is consistent with the structure of the designed co-polymer, i.e., PEG-grafted chitosan.

Crystalline and thermal properties of CS-g-mPEGs

The typical XRD patterns of chitosan, mPEG-CHO and CS-g-mPEGs are shown in Fig. 2. There is no crystalline peak observed at 2θ values of 10–40° in the XRD patterns of chitosan. mPEG-CHO has two strong characteristic crystalline peaks at 2θ values of 21.9° and 26.8° and two weak characteristic crystalline peaks at 2θ values of 30° and 31°. CS-g-mPEGs also have two obvious characteristic crystalline

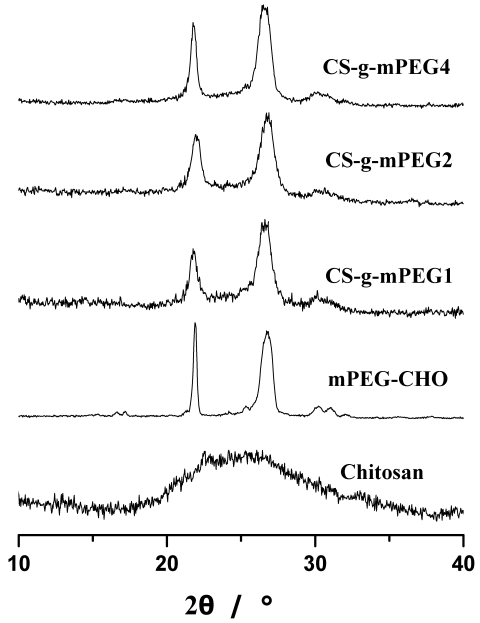

Figure 2. XRD spectra of chitosan, mPEG-CHO, CS-g-mPEG1, CS-g-mPEG2 and CS-g-mPEG4. DS of CS-g-mPEG1, CS-g-mPEG2 and CS-g-mPEG4 is 6, 14 and 22%, respectively. All the samples were measured at a voltage of 20 kV, current of 20 mA, scan range of 3–45° and scan interval of 0.0334°.

peaks at 2θ values of 21.9° and 26.8° and become stronger with increasing DS, and the peaks at 2θ values of 30° and 31° are inconspicuous.

The thermal properties of chitosan and CS-g-mPEGs were determined by DSC, and the results are shown in Table 2. Because chitosan can absorb water easily, the second run method is adopted to eliminate the effects of water. An endothermic peak is found for CS-g-mPEG samples at about 50°C during the second heating run and becomes stronger and shifts to higher temperature with DS of CS-g-mPEGs increasing. There are a lot of investigations on the glass transition temperature (T_g) of chitosan but there has been no consistent result yet [43–45]. As shown in Table 2, neither the glass transition temperature nor the fusion temperature (T_m) of chitosan moieties was detected during the second run. This phenomenon is consistent with the results of XRD.

The thermal weight-loss curves of chitosan and CS-g-mPEGs are shown in Fig. 3. It can be seen that chitosan has two obvious weight-loss phases. The range from 35 to 130°C is the first weight-loss phase and the maximal weight-loss temperature is 70°C, which is caused by loss of water. The second quickly weight-loss from 260 to 350°C with a maximal weight-loss temperature of 320°C is caused by the dehydration of sugar unit, bond cleavage of main chain and decomposition of acetyl and deacetylated units. The weight-loss process of CS-g-mPEGs has two phases and it is obviously distinct from the weight-loss curve of chitosan. The first quick

Table 2.
Melting temperature of co-polymers

Polymer	DS[a] (%)	T_m (°C)
Chitosan (5.6 kDa)		_[b]
mPEG (2 kDa)		60
CS-g-mPEG1	6	48
CS-g-mPEG2	14	51
CS-g-mPEG3	18	52
CS-g-mPEG4	22	54

DSC data of chitosan and CS-g-mPEG were obtained from the second run. All the samples were approximately 5 mg. All the measurements were carried out at a heating (cooling) rate of 10°C/min from −50°C to 200°C.

[a] DS means the degree of substitution of mPEG to monosaccharide residue of chitosan determined with a Carlo Erba 1106 element analyzer.

[b] Not detected.

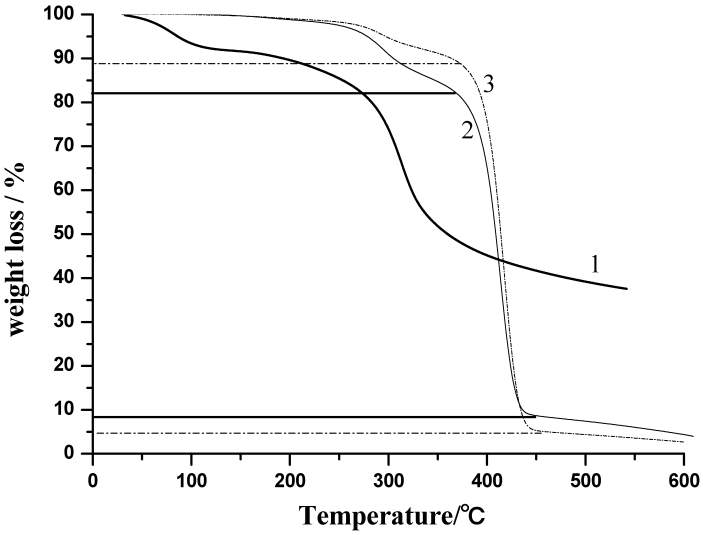

Figure 3. TG curves of chitosan (1), CS-g-mPEG2 (2), CS-g-mPEG4 (3). DS of CS-g-mPEG2 and CS-g-mPEG4 was 14 and 22%, respectively. The thermal weight-loss analysis of chitosan and CS-g-mPEG were carried out with a thermogravimetric apparatus (Perkin Elmer Pyris 6 TGA) at a heating rate of 10°C/min. All the samples were approximately 11 mg.

weight loss of CS-g-mPEGs at 320°C is caused by the decomposition of chitosan moieties and the second one at 410°C is assigned to the mPEG moieties.

Hydrodynamic behavior of CS-g-mPEGs in aqueous solution

Chitosan does not dissolve in deionized H_2O, but CS-g-mPEGs do and spontaneously form nanometer-sized aggregates by strong intermolecular hydrogen bonds between chitosan moieties. The size distribution and morphology of CS-g-mPEG4

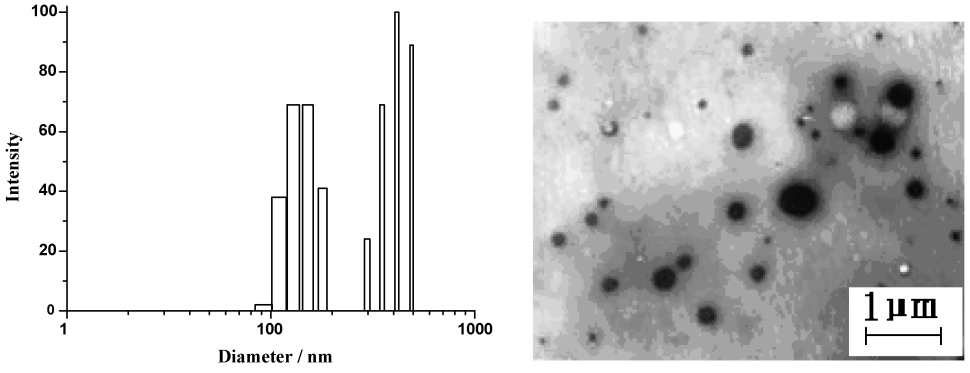

Figure 4. Size distribution (A) and TEM image (B) of the CS-g-mPEG4 aggregates in deionized H_2O. DS of CS-g-mPEG4 was 22%. The concentration of CS-g-mPEG4 in deionized H_2O was 5 mg/ml.

aggregates in deionized H_2O are shown in Fig. 4. It can be seen that the CS-g-mPEG4 aggregates take on a spherical structure with a size $<$ 500 nm and a polydispersion index of 0.312. The results of LPSA indicate that the size of the PEG-g-mPEG particles in deionized H_2O decreases with increasing DS. The PEG-g-mPEG2 and PEG-g-mPEG3 represent larger particle size, 550 nm and 500 nm in deionized H_2O, respectively, and PEG-g-mPEG1 is difficult to disperse into deionized H_2O.

The viscometric properties of the PEG-g-mPEG aggregates aqueous solution are shown in Fig. 5. The dilute behavior of common colloid solutions that η_{sp}/C decreases with decreasing the colloid concentration was observed for PEG-g-mPEG aggregates aqueous solutions. η_{sp}/C of CS-g-mPEG2 in deionized H_2O is slightly greater than CS-g-mPEG4 in deionized H_2O and approaches to the latter with decreasing the concentration.

The influences of the CS-g-mPEG concentration on the reduced viscosity in 2% acetic acid solution are shown in Fig. 6. It can be seen that η_{sp}/C of CS-g-mPEGs in acetic acid solution is greater than that of CS-g-mPEGs in deionized H_2O but lower than that of chitosan in acetic acid solution at the same concentration. Figure 6 shows chitosan in acetic acid solution represents typical polyelectrolyte viscometric behavior in that η_{sp}/C decreases with decreasing concentration in the higher concentration region but increases with the decrease of concentration in the lower concentration region (below 0.01 g/ml), which is assigned to the polyelectrolyte effect because of the ionization extent increasing upon dilution. PEG grafting on chitosan impacts the viscometric behavior largely as shown in Fig. 6. That is, the η_{sp}/C values of CS-g-mPEGs in acetic acid solution are nearly constant in the greater concentration range of 10–30 mg/ml. The polyelectrolyte effect in the lower concentration range becomes weak while DS of CS-g-mPEGs increases and disappears when the DS is 22%. The results of investigating the charge effect show that the zeta potential of CS-g-mPEGs in acid solution is

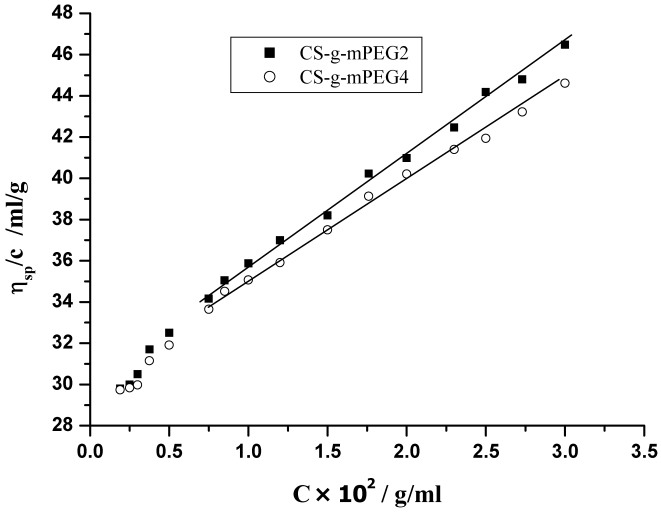

Figure 5. Influences of the CS-g-mPEG concentration on the reduced viscosity of CS-g-mPEG in deionized H_2O. DS of CS-g-mPEG2 and CS-g-mPEG4 was 14 and 22%, respectively.

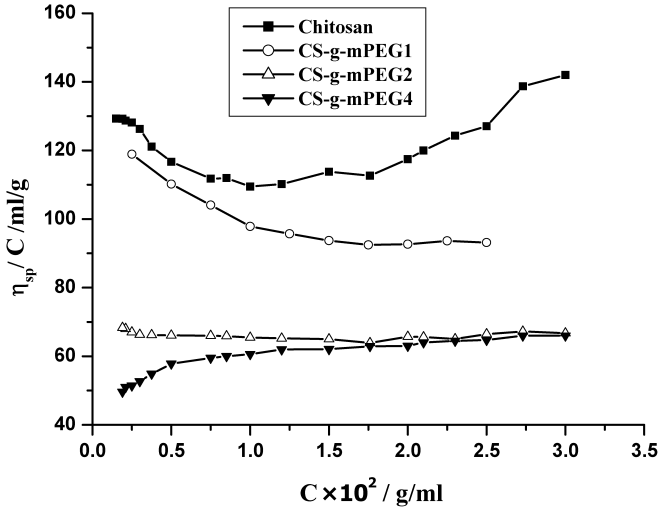

Figure 6. Influences of the CS-g-mPEG concentration on the reduced viscosity of polymer in 2% acetic acid solution. DS of CS-g-mPEG1, CS-g-mPEG2 and CS-g-mPEG4 was 6, 14 and 22%, respectively.

decreased with the increment of DS, i.e., the zeta potential is 37.7 ± 0.9 (chitosan), 32.4 ± 1.2 (CS-g-mPEG1), 18.1 ± 1.4 (CS-g-mPEG2), 13.2 ± 1.1 (CS-g-mPEG3) and 7.4 ± 1.0 (CS-g-mPEG4), respectively.

The influences of C_{NaCl} on η_{sp}/C value of CS-g-mPEGs in 2% acetic acid solution are exhibited in Fig. 7. The η_{sp}/C value of chitosan in acetic acid solution sharply drops firstly and then increases with C_{NaCl} increasing. Finally, chitosan deposites out of the solution at C_{NaCl} of 1.05 mol/l. Although similar changes in η_{sp}/C value

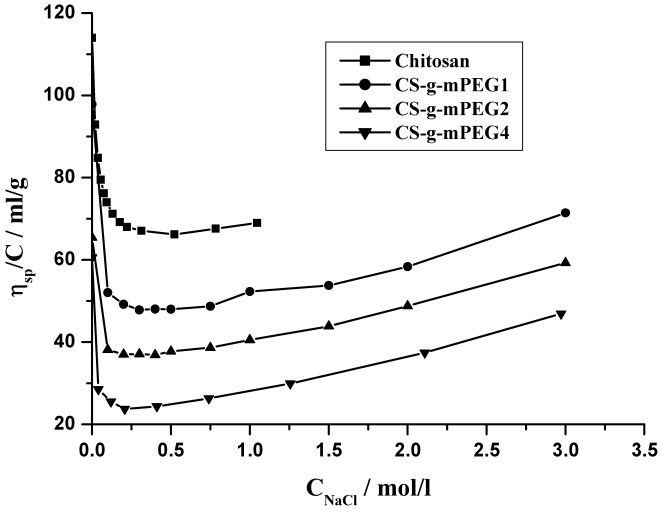

Figure 7. Influences of C_{NaCl} on the reduced viscosity of CS-g-mPEG in 2% acetic acid solution. The concentrations of chitosan and CS-g-mPEG in 2% acetic acid solution were 10 mg/ml. DS of CS-g-mPEG1, CS-g-mPEG2 and CS-g-mPEG4 was 6, 14 and 22%, respectively.

with increasing C_{NaCl} are observed for CS-g-mPEGs in acetic acid solutions, all the CS-g-mPEGs samples in acetic acid solution are stable at higher C_{NaCl} and do not precipitate out of the solution at $C_{NaCl} = 3.0$ mol/l.

Properties of CS-g-mPEGs ion gelation NPs

Chitosan NPs can be formed by coacervation of sodium tripolyphosphate (TPP) under certain conditions [46]. Because of the protonated amine groups in the CS-g-mPEGs, CS-g-mPEG NPs can be prepared by the same method. The size distribution and morphology of the CS-g-mPEG NPs are shown in Fig. 8. The result indicates that the CS-g-mPEG4 NPs take on a spherical structure, the average size is approximately 100 nm and the polydispersion index is 0.242.

The TPP dosage plays a very important role on the stability and the particle size of CS-g-mPEG NPs. As shown in Fig. 9, the CS-g-mPEG NPs were formed at a CS-g-mPEG4/TPP (mol/mol) ratio of 10 with an average size of 112 nm. With the TPP dosage increasing, the size of the CS-g-mPEG4 NPs increases.

DISCUSSION

The XRD and DSC results above obviously show the crystal phase of mPEG segments exists in CS-g-mPEGs solid and increases with increasing DS, which means the microphase separation morphology of CS-g-mPEGs solid with mPEG crystal and CS domains. From the TGA curves, it can be calculated that there is about 50% left at 440°C for CS, and 6% and 9% left, respectively, for CS-g-mPEG4 and

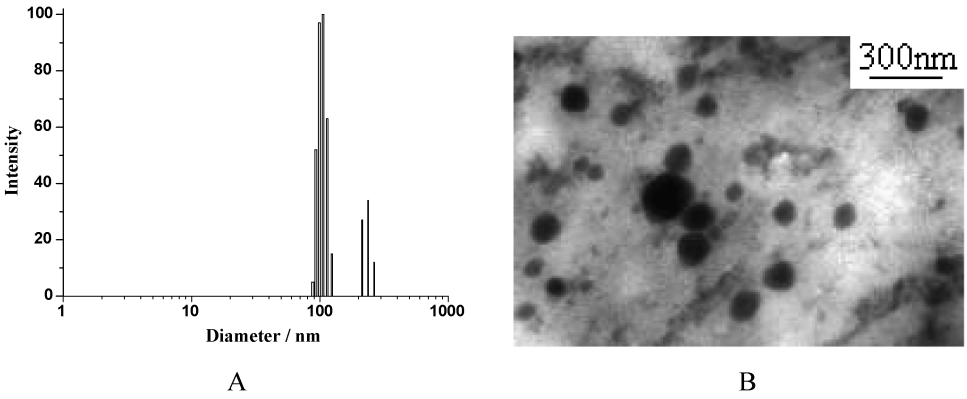

Figure 8. TEM image of the CS-g-mPEG NPs prepared by the ion gelation method. The CS-g-mPEG4 concentration was 10 mg/ml and the ratio of CS-g-mPEG/TPP (mol/mol) was 10. The system was stirred by magnetic stirring at ambient temperature for 10 min.

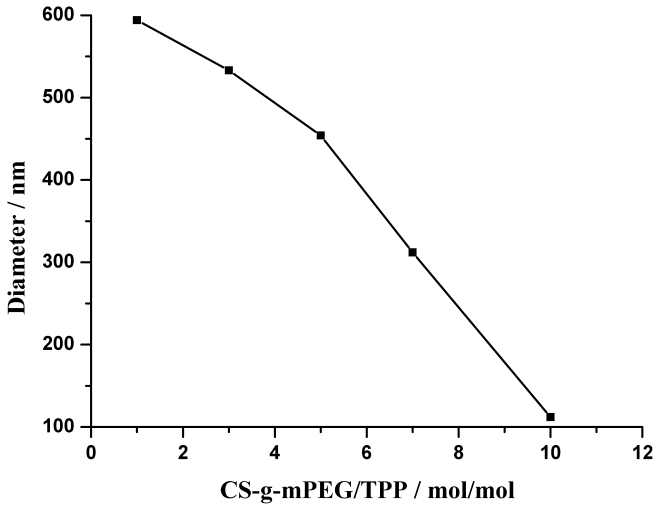

Figure 9. Influences of the ratio of CS-g-mPEG/TPP (mol/mol) on the size of NPs. The concentration of CS-g-mPEG4 was 10 mg/ml. The system was stirred under magnetic stirring at ambient temperature for 10 min.

CS-g-mPEG2 when exclude the water content. The CS content of CS-g-mPEG4 and CS-g-mPEG2 is, respectively, 27% and 36%. These results indicate that the introduction of PEG on CS side-chains improves the thermal decomposition. That means the mPEG segments destroy part of the hydrogen bonds between CS chains and part of the CS domains. The CS domains are a composite of strong inter- or intra-molecular hydrogen bond aggregation between glucosamine units of CS, which can be destroyed by the positively charged action of $-NH_2$ groups in acidic aqueous media. When CS-g-mPEGs are dispersed in deionized H_2O, mPEG crystal domains are dissolved and the PEG segments stretch into the water, but the CS

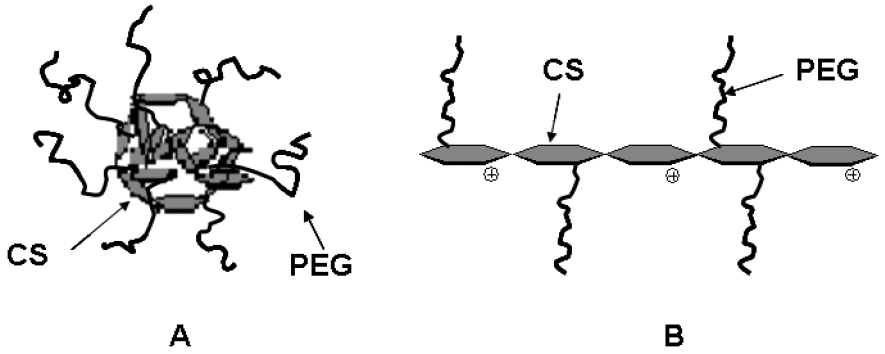

Figure 10. Aggregation state in deionized H_2O (A) and dissociation state in acid aqueous solutions (B) of CS-g-mPEGs.

domains keep the hydrogen bonds aggregation state. As a result, the self-assembly nanoparticles with PEG shell covering CS aggregation core are formed in water solution, as shown in Fig. 10A. In acid aqueous solutions, CS domains will disaggregate because the $-NH_2$ are positive charged and stretch with grafted PEG hydrophilic chains, as shown in Fig. 10B.

The hydrophilic and flexible PEG chains have rapid chain motion and a large excluded volume, which provide the stability of the CS-g-mPEGs particles in deionized H_2O by decreasing the interaction between the CS cores, i.e., decreasing the frictional resistance between the particles; therefore, the dispersions of spheric CS-g-mPEGs particles in deionized H_2O represent lower viscosity. The small difference in η_{sp}/C between CS-g-mPEG2 and CS-g-mPEG4 particles dispersions in deionized H_2O is induced just by the particle size difference.

The stretching molecular conformation of CS-g-mPEGs in acetic acid solution has bigger hydrodynamic resistance and the protonated amine groups of chitosan causes the intramolecular electrostatic repulsion, so η_{sp}/C of CS-g-mPEGs in acetic acid solution is greater than that of CS-g-mPEGs in deionized H_2O. But compared to chitosan, the CS-g-mPEGs with relatively fewer chitosan moieties and protonated amine groups, as well as the existence of the mPEG flexible chain in CS-g-mPEGs make the electrostatic repulsion of macromolecular weaker. Therefore, the η_{sp}/C value of CS-g-mPEGs in acid solution is lower than that of chitosan in acetic acid solution. It is because of the screen effect of the large excluded volume of PEG chains covering the CS chains and the interaction between the CS-g-mPEGs that the typical polyelectrolyte effect of polyelectrolyte solution upon dilution gradually disappears with increasing PEG content for CS-g-mPEGs. The results of the zeta potential further confirm that the screen effect of PEG chains increases with increasing DS.

The screen effect of the large excluded volume of PEG chains also provide better salt-resistant properties of CS-g-mPEGs, as seen in Fig. 7. With an increase of C_{NaCl}, the shielding effect of Cl^- on the charges in macromolecular chains results in the shrinking of the whole molecule, which reduces the hydrodynamic volume

and η_{sp}/C of chitosan in acetic acid solution. When C_{NaCl} is greater than 0.5 mol/l, the effective charge density in the macromolecular chain is insufficient to restrain the aggregation of chitosan chains, which leads to the aggregates and the increase in η_{sp}/C value. Once C_{NaCl} is greater than 1.05 mol/l, chitosan will precipitate out of the solution. Compared to chitosan, CS-g-mPEGs in acetic acid solution are more stable at greater C_{NaCl} because the PEG chains can prevent the aggregating extent.

Although the PEG chains screen the interaction between the CS chains, they do not affect the complexation property of CS with negatively charged compounds by electrostatic interaction. CS-g-mPEGs can form nanoparticles with TPP and the PEG chains also provide protection to the complex nanoparticles. Therefore, the CS-g-mPEG self-assembly nanoparticles in aqueous solution with lower viscosity, higher salt-resistant property and good stability have potential application in drug delivery.

CONCLUSIONS

CS-g-mPEGs with different degrees of substitution have been synthesized and the hydrodynamic and aggregation properties of CS-g-mPEGs in aqueous solutions have been studied combined with the crystaline and thermal analysis of CS-g-mPEGs solid. CS-g-mPEGs solids represent microphase separation morphology with mPEG crystal and CS domains coexistence, and the dissolution of PEG crystal in deionized H_2O leads to the dispersion of CS-g-mPEGs solids into water and formation of CS-g-mPEGs particles with PEG shell and CS core. The screen effect of the large excluded volume of hydrophilic PEG chains leads to lower viscosity solutions of CS-g-mPEGs in aqueous solutions and provide better salt-resistant property of CS-g-mPEGs, whereas the grafted PEG chains do not affect the complexision property of CS with negative charged compounds by electrostatic interaction and provide protection for the oppositely charge complexes.

Acknowledgements

This work was supported by Program for New Century Excellent Talents in University of China and Programme of Introducing Talents of Discipline to Universities (No. B06006).

REFERENCES

1. M. F. A. Goosen, *Applications of Chitin and Chitosan*. Technomic, Lancaster, PA (1997).
2. A. Bernkop-Schnurch, *Int. J. Pharm.* **194**, 1 (2000).
3. Y. Sudhakar, K. Kuotsu and A. K. Bandyopadhyay, *J. Control. Release* **114**, 15 (2006).
4. R. Jayakumar, M. Prabaharan, R. L. Reis and J. F. Mano, *Carbohydr. Polym.* **62**, 142 (2005).
5. A. Bernkop-Schnürch and C. E. Kast, *Adv. Drug Deliv. Rev.* **52**, 127 (2001).
6. S. M. van der Merwe, J. C. Verhoef, J. H. M. Verheijden, A. F. Kotzé and H. E. Junginger, *Eur. J. Pharm. Biopharm.* **58**, 225 (2004).

7. H. Sashiwa and S. Aiba, *Prog. Polym. Sci.* **29**, 887 (2004).
8. P. Dung, M. Milas, M. Rinaudo and R. Desbrières, *J. Carbohydr. Polym.* **24**, 209 (1994).
9. C. Prego, D. Torres, E. Fernandez-Megia, R. Novoa-Carballal, E. Quiñoá and M. J. Alonso, *J. Control. Rel*. **111**, 299 (2006).
10. M. Zhang, X. H. Li, Y. D. Gong, N. M. Zhao and X. F. Zhang, *Biomaterials* **23**, 2641 (2002).
11. S. J. Lee, S. S. Kim and Y. M. Lee, *Carbohydr. Polym.* **41**, 197 (2000).
12. A. D. Pozzo, L. Vanini, M. Fagnoni, M. Guerrini, A. D. Benedittis and R. A. A. Muzzarelli, *Carbohydr. Polym.* **42**, 201 (2000).
13. N. Bhattarai, F. A. Matsen and M. Zhang, *Macromol. Biosci.* **5**, 107 (2005).
14. F. Lebouc, I. Dez, J. Desbrières, L. Picton and P. J. Made, *Polymer* **46**, 639 (2005).
15. S. R. Mao, X. T. Shuai, F. Ungera, M. Wittmara, X. L. Xie and T. Kissel, *Biomaterials* **26**, 6343 (2005).
16. M. M. Amiji, *Carbohydr. Polym.* **32**, 193 (1997).
17. T. Ouchi, H. Nishizawa and Y. Ohya, *Polymer* **39**, 5171 (1998).
18. T. Muslim, M. Morimoto, H. Saimoto, Y. Okamoto, S. Minami and Y. Shigemasa, *Carbohydr. Polym.* **46**, 323 (2001).
19. S. J. Lee, S. S. Kim and Y. M. Lee, *Carbohydr. Polym.* **41**, 197 (2000).
20. M. Rutnakornpituk, P. Ngamdee and P. Phinyocheep, *Polymer* **46**, 9742 (2005).
21. P. Chan, M. Kurisawa, J. E. Chung and Y. Y. Yang, *Biomaterials* **28**, 540 (2007).
22. Y. Q. Hu, H. L. Jiang, C. N. Xu, Y. J. Wang and K. J. Zhu, *Carbohyd. Polym.* **61**, 472 (2005).
23. M. Sugimoto, M. Morimoto, H. Sashiwa, H. Saimoto and Y. Shigemasa, *Carbohydr. Polym.* **36**, 49 (1998).
24. M. D. Bentley, M. J. Roberts and J. M. Harris, *J. Pharm. Sci.* **87**, 1446 (1998).
25. R. Makuska and N. Gorochovceva, *Carbohydr. Polym.* **64**, 319 (2006).
26. I. K. Park, T. H. Kim, S. I. Kim, Y. H. Park, W. J. Kimc, T. Akaike and C. S. Cho, *Int. J. Pharm.* **257**, 103 (2003).
27. S. Mao, X. Shuai, F. Unger, M. Wittmar, X. L. Xie and T. Kissel, *Biomaterials* **26**, 6343 (2005).
28. Y. M. Dong, Y. H. Ruan and H. W. Wang, *J. Appl. Polym. Sci.* **4**, 1553 (2004).
29. Y. Ohya, R. Cai, H. Nishizawa, K. Hara and T. Ouchi, *S.T.P. Pharma. Sci.* **10**, 77 (2000).
30. H. Saito, X. Wu, J. M. Harris and A. S. Hoffman, *Macromol. Rapid Commun.* **18**, 547 (1997).
31. P. Calvo, C. Remuńan-Löpez, J. L. Vila-Jato and M. J. Alonso, *J. Appl. Polym. Sci.* **63**, 125 (1997).
32. O. Felt, P. Buri and R. Gurny, *Drug Dev. Ind. Pharm.* **24**, 979 (1998).
33. Y. Wu, W. Yang, C. Wang, J. Hu and S. Fu, *Int. J. Pharm.* **295**, 235 (2005).
34. Y. Xu and Y. Du, *Int. J. Pharm.* **250**, 215 (2003).
35. C. Prego, M. Garcí, D. Torres and M. J. Alonso, *J. Control. Rel.* **101**, 151 (2005).
36. F. C. MacLaughlin, R. J. Mumper and J. J. Wang, *J. Control. Rel*. **56**, 259 (1998).
37. H. Q. Mao, K. Roy, V. L. Troung-Le, K. A. Janes, K. Y. Lin, Y. Wang, J. T. August and K. W. Leong, *J. Control. Rel.* **70**, 399 (2001).
38. I. K. Park, T. H. Kim, Y. H. Park, B. A. Shin, E. S. Choi, E. H. Chowdhury, T. Akaike and C. S. Cho, *J. Control. Rel.* **76**, 349 (2001).
39. Y. Aktasü, M. Yemisc and K. Andrieux, *Bioconjug. Chem.* **16**, 1503 (2005).
40. J. Berger, M. Reist, J. M. Mayer, O. Felt and R. Gurny, *Eur. J. Pharm. Biopharm.* **57**, 35 (2004).
41. S. C. W. Richardson, H. J. V. Kolbe and R. Duncan, *Int. J. Pharm*. **178**, 231 (1999).
42. Y. Q. Hu, H. L. Jiang, C. N. Xu, Y. J. Wang and K. J. Zhu, *Carbohydr. Polym.* **61**, 472 (2005).
43. J. S. Ahn, H. K. Choi and C. S. Cho, *Biomaterials* **22**, 923 (2001).
44. K. Sakurai, T. Maegauna and T. Takashi, *Polymer* **41**, 7051 (2000).
45. Y. M. Dong, Y. H. Ruan and H. W. Wang, *J. Appl. Polym. Sci.* **4**, 1553 (2004).
46. Y. Pan, Y. J. Li, H. Y. Zhao, J. M. Zheng, H. Xu, G. Wei, J. S. Hao and F. D. Cui, *Int. J. Pharm.* **249**, 139 (2002).